Received: 27 April 2019 | Revised: 9 July 2019 | Accepted: 10 July 2019
DOI: 10.1002/jccs.201900163

SPECIAL ISSUE PAPER

JOURNAL OF THE CHINESE CHEMICAL SOCIETY

Synthesis, photoluminescence, and electroluminescence characterization of double tetraphenylethene-tethered BODIPY luminogens

Chiun-Jen Yang[1] | **Jian Haur Lee**[2] | **Chin-Ti Chen**[1,2]

[1]Department of Applied Chemistry, National Chiao Tung University, Hsinchu, Taiwan, ROC
[2]Institute of Chemistry, Academia Sinica, Taipei, Taiwan, ROC

Correspondence
Chin-Ti Chen, Institute of Chemistry, Academia Sinica, Taipei 11529, Taiwan, ROC.
Email: chintchen@gate.sinica.edu.tw

Funding information
Innovative Materials and Analysis Technology Exploration Program, Academia Sinica, Grant/Award Number: AS-iMATE-108-33; Ministry of Science and Technology, Taiwan, Grant/Award Number: MOST 106-2113-M-001-016-MY3; National Chiao Tung University

Three double tetraphenylethene (TPE)-tethered 4-difluoro-4-bora-3*a*,4*a*-diaza-*s*-indance (BODIPY) fluorophores, **35TPEBODP**, **88TPEBODP**, and **26TPEBODP**, have been synthesized and characterized. The green **35TPEBODP** with deep red fluorescence shows serious thermal decomposition in the purification process of sublimation, which prohibits its test for an organic light-emitting diode (OLED) fabricated by the vacuum–thermal evaporation process. The tethered TPE is attached to BODIPY at three different positions, resulting in different photoluminescence (emission wavelength and quantum yield) and electroluminescence (EL). Different from TPE-tethered BODIPY fluorophores reported in literature, none of the BODIPY fluorophores studied here exhibits aggregation-induced emission (AIE), aggregation-induced enhanced emission (AIEE), or twisted intramolecular charge transfer (TICT) characteristics. Although solution (10^{-5} M THF) photoluminescence quantum yields (ϕs) are relatively high at 78%, 68%, and 86% for **35TPEBODP**, **88TPEBODP**, and **26TPEBODP**, respectively, which are all higher than 41% of **PhBODP** (a non-TPE-tethered BODIPY), the ϕ is significantly decreased to 1–6% in 5 wt% dopant polystyrene thin film or as a solid powder, except for 13% of **26TPEBODP**. Therefore, due to the low ϕ of dopant thin film or solid powder, either dopant or nondopant OLEDs exhibit inferior external quantum efficiency (EQE) and intensity of EL. The best OLED in this study is the **26TPEBODP** device, and its EQE reaches 1.3%, and the highest EL intensity is approximately 1,600 cd/m^2.

KEYWORDS
BODIPY, electroluminescence, OLED, photoluminescence, tetraphenylethene

1 | INTRODUCTION

4,4-Difluoro-4-bora-3*a*,4*a*-diaza-*s*-indance (BODIPY) is boron difluoride chelated by a π-conjugated dipyrromethene, exhibiting an intense fluorescence in solution. For example, one of the BODIPY derivatives, PM 546 (Scheme 1), a commercially available green laser dye, has been reported with a $\lambda_{max}{}^{em}$ of 506 nm and 95% of photoluminescence quantum yield (PLQY) in methanol solution.[1] However, these highly fluorescent BODIPY derivatives often suffer from serious emission quenching in solid state, causing diminishingly small PLQY and limiting their applications in organic optoelectronics, such as organic lighting-emitting diodes (OLEDs).

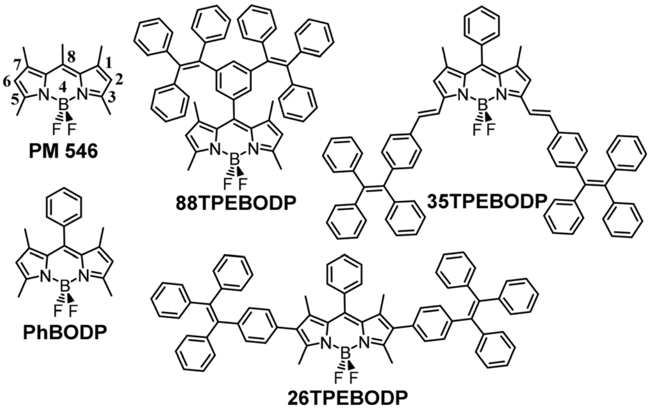

SCHEME 1 Chemical structure of BODIPY luminogens in this study

Tetraphenylethene (TPE) has been known as one of the most potent chemical moieties to alleviate emission quenching in solid state through the so-called effect of aggregation-induced emission (AIE).[2,3] In light of the AIE, a chemical structure hybrid of TPE and BODIPY seems to be a logical approach to overcome the problem of emission quenching in solid state. In fact, there are already several reports of TPE-decorated BOPIPY luminogens, including **26TPEBODP** (Scheme 1), in the literature.[4–9] However, these TPE-decorated BOPIPY luminogens show moderate to intense emission in organic solutions without water. Therefore, instead of AIE, aggregation-induced enhanced emission (AIEE) or even aggregation-caused quenching (ACQ) is probably a better term for characterizing such TPE-containing luminogens. Furthermore, compared with TPE-undecorated BODIPY, some of these TPE-containing BODIPY luminogens exhibit color-shifted red fluorescence in solid state, simply due to the ππ interaction of molecular stacking, or it is ascribed to a twisted intramolecular charge transfer (TICT).[8,10] AIEE or ACQ, as well as ππ interaction or TICT, of TPE-decorated BOPIPY luminogens hinges on the position (and maybe the number) of the decorated (or "tethered" used in this study) TPE moiety. Nevertheless, except for one case, none of them has been applied for OLEDs. Only the triple TPE-tethered BODIPYs have been fabricated as a polymer-blended OLED, a dopant-based device, from a solution process,[9] rather than a vacuum–thermal deposition one.

Accordingly, in this study, we have synthesized and characterized two new double TPE-decorated BOPIPY luminogens, **88TPEBODP** and **35TPEBODP** (Scheme 1), together with previously known **26TPEBODP**, which is also a double TPE-tethered BODIPY.[5,7] In addition, for the purpose of comparison, **PhBODP**, a non-TPE-tethered BODIPY, was also adopted in the dopant and nondopant OLEDs, which were all fabricated by the vacuum–thermal deposition process. We try to study the electroluminescence (EL) and understand or clarify the photoluminescence (PL) of these BODIPYs, of which double-tethered TPE are at three different positions, that is, 8 and 8, 3 and 5, and 2 and 6.

2 | RESULTS AND DISCUSSIONS

2.1 | Synthesis

Previously known **PhBODP** and **26TPEBODP** were readily prepared based on procedures described in the literature.[5,7,11] The synthesis of **88TPEBODP** is shown in Scheme 2. A key intermedia, 3,5-bis[1,2,2-triphenylvinyl]benzaldehyde, an unknown new compound, was synthesized by the Suzuki cross coupling of bromotriphenylethylene and 3,5-bis(pinacolboranyl)benzaldehyde, which was synthesized following a conventional procedure of a two-step reaction from tribrobenzene in moderate yields.

The synthesis of **35TPEBODP** is shown in Scheme 3. It was prepared using microwave heating via the Knövenagel condensation of **PhBODP** and 4-(1,2,2-triphenylvinyl)benzaldehyde, which was facilely synthesized following modified procedures described in the literature,[12,13] and its structural characterization was consistent with that given in the literature.[12]

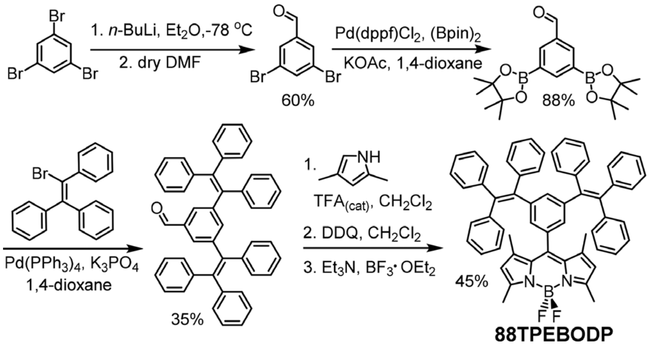

SCHEME 2 Synthesis of **88TPEBODP**

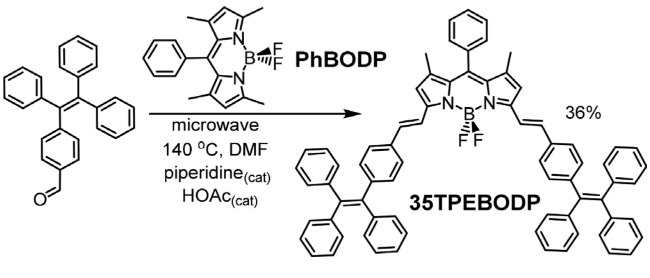

SCHEME 3 Synthesis of **35TPEBODP**

2.2 | Thermal stability

Thermal stability is one of the vital factors that validate the feasibility of vacuum–thermal deposition in device fabrication. Figure 1 illustrates the TGA thermograms of three TPE-tethered BODIPY compounds in this study.

Although the TGA results show similar thermal stability of the three BODIPY compounds, the purification process of gradient sublimation afforded **35TPEBODP** with serious decomposition because the intact **35TPEBODP** should show a dark green color (see Figure 2). Such a result mostly prohibits its OLED fabrication with a vacuum–thermal deposition process. We infer that the more extended molecular shape and the flexible vinyl connection of **35TPEBODP** reduces the volatility of the material, which needs a higher temperature to be sublimed and causes extensive decomposition of the material. The extended molecular shape of **26TPEBODP** also hinders the evaporation process of sublimation. A time period almost three to four times longer was required to complete the purification process. This also resulted in a prolonged OLED fabrication process, and a partial thermal decomposition was also observed for **26TPEBODP**.

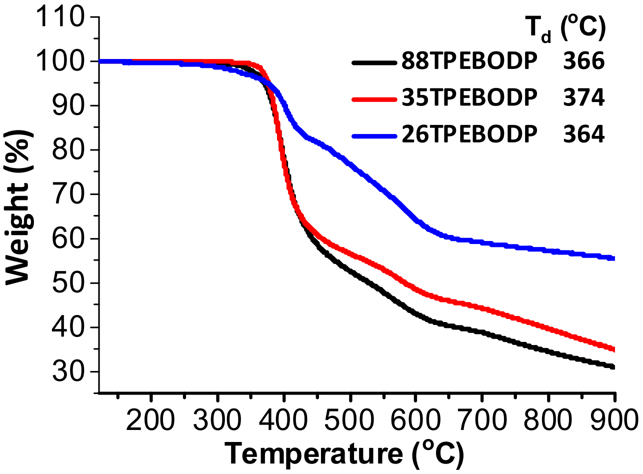

FIGURE 1 TGA thermograms of three TPE-tethered BODIPY compounds

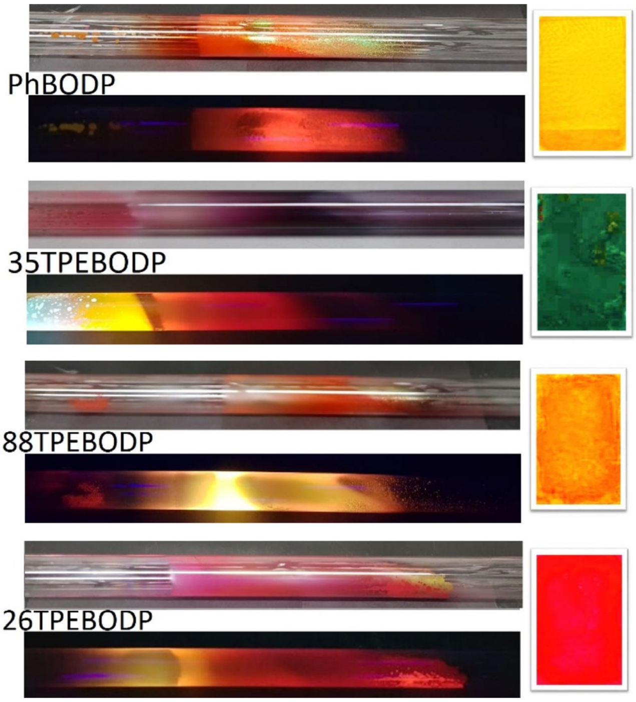

FIGURE 2 Photograph (under visible light and 366 nm UV light) of gradient sublimation of **PhBODP** and three TPE-tethered BODIPY compounds. Color pictures on the right are the corresponding 5 wt% dopant samples in polystyrene thin film

2.3 | Photoluminescence characterization

2.3.1 | 35TPEBODP

Solution PL of **35TPEBODP** is concentration dependent. First, compared with 506 nm of PM546 or 519 nm of **PhBODP**, **35TPEBODP** exhibits a significantly red-shifted λ_{max}^{em} of 675 and 725 nm in THF solution of a concentration of 10^{-5} and 10^{-3} M, respectively. This is mainly due to the effective extension of the π conjugation of the BODIPY core via a vinyl group connected to TPE units. At a high concentration of 10^{-3} M, the **35TPEBODP** THF solution exhibits a simple and broad deep red emission spectra with a λ_{max}^{em} of around 725 nm at a water volume fraction (vol%) of 0%, 20%, and 40% and slightly red-shifted to approximately 750 nm at water vol% of 60, 70, and 80%, respectively (Figure 3). Regarding fluorescence intensity, 60% is the common water vol% at which the brightness of the fluorescence photograph and the intensity of the fluorescence spectra become significantly decreased. We can infer that 60% is the water vol% at the beginning of the formation of the aggregate of **35TPEBODP** in THF solution. Such a PL behavior is a typical ACQ, which is neither AIE nor AIEE.

At a low concentration of 10^{-5} M, spectra become quite different (Figure 4). First, there is an emission band with a λ_{max}^{em} of around 735–740 nm, which is not observed in the solution with a high concentration of 10^{-3} M. Based on a vibronic shoulder band observed in the absorption spectra (not shown here), this emission band can be attributed to the vibronic emission of the main emission with λ_{max}^{em} of around 677 nm at water vol% of 0, 20, and 40%. These are all blue-shifted spectra compared with those of high concentration (10^{-3} M). Unlike those of high concentrations of 10^{-3} M, these fluorescence intensities (water vol% of 0, 20, and 40%) are almost same. The more diluted concentration prevents the molecules of **35TPEBODP** from ππ interaction, rendering better-resolved, similar intensity, and blue-shifted spectra. Nevertheless, similar to that of a high concentration

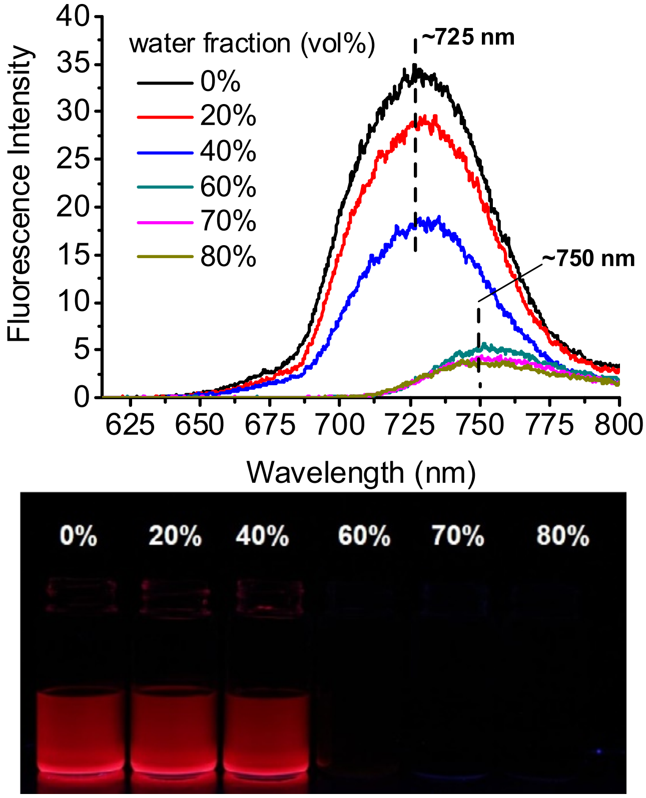

FIGURE 3 Fluorescence spectra (top) and fluorescence photograph (bottom) of **35TPEBODP** in THF solution (10^{-3} M) with various water volume fractions. Fluorescence spectra were recorded with a 600 nm excitation wavelength. Fluorescence photographs were taken under a UV illumination at 366 nm

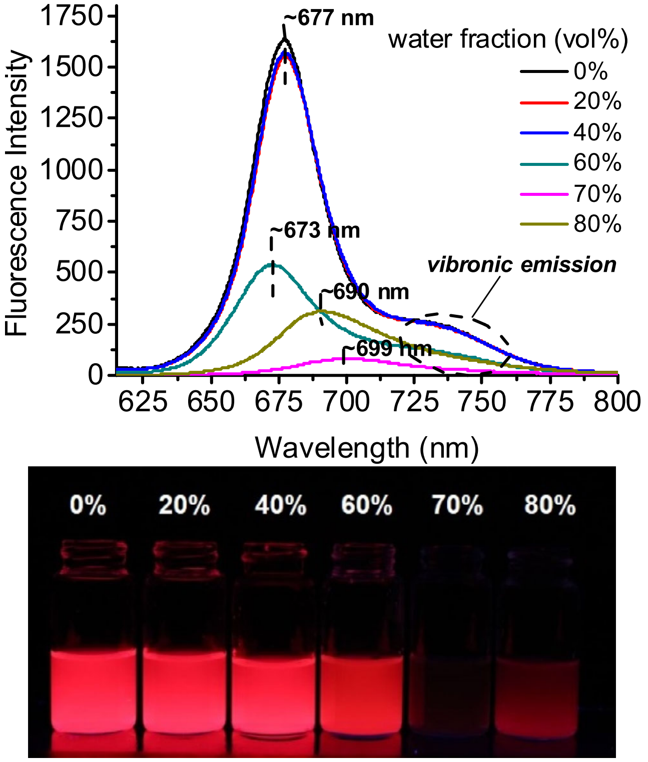

FIGURE 4 Fluorescence spectra (top) and fluorescence photograph (bottom) of **35TPEBODP** in THF solution (10^{-5} M) with various water volume fractions. Fluorescence spectra were recorded with a 600 nm excitation wavelength. Fluorescence photographs were taken under a UV illumination at 366 nm

solution, the intensity of the emission decreases significantly when the water vol% increases to 60%, although the wavelength is slightly blue-shifted. The intensity decreases further, and the wavelength of λ_{max}^{em} is red-shifted to approximately 699 nm with a higher water vol% of 70%. However, at water vol% of 80%, such a red emission is blue-shifted slightly to approximately 690 nm (in terms of energy, the difference between 690 and 699 nm is rather small), and the intensity of the emission becomes moderately stronger (Figure 4). Similar to that of high concentration, we suggest that the solution PL of **35TPEBODP** exhibits ACQ even at diluted concentrations of 10^{-5} M. The two vinyl-connected TPE units at the 3, 5 position cannot overcome the molecular ππ interaction that quenches the fluorescence of **35TPEBODP**.

2.3.2 | 88TPEBODP

The solution PL of **88TPEBODP** is also concentration dependent. At a high concentration of 10^{-3} M, **88TPEBODP** THF solution exhibits green emission λ_{max}^{em} of around 543 nm with 0, 20, and 40% of water vol% and progressively red-shifts to 550 nm with 60, 70, and 80% water vol% (Figure 5), of which fluorescence intensity is displayed in a log scale for clarity. However, at high water vol %, a new emission band with a longer wavelength of around 625 nm, as well as a new emission band with shorter wavelength between 510 and 525 nm, appears. Different from the literature precedents,[8,10] we attribute such new emission bands to a J-type and H-type aggregate of **88TPEBODP** for the longer and shorter wavelengths, respectively. Particularly for water vol% of 70 and 80%, the emerging new emission band with a λ_{max}^{em} of approximately 620 nm, together with an intensity-declined fluorescence of around 550 nm, results in a visible fluorescence color change from green to orange (Figure 5).

At a low concentration of 10^{-5} M, the **88TPEBODP** THF solution exhibits much simpler green emission spectra, showing a λ_{max}^{em} of around 516 nm at water vol% of 0, 20, 40, and 60%. A weaker emission band with λ_{max}^{em} of around 550 nm can be assigned to the vibronic emission side-band of λ_{max}^{em} of around 516 nm. All these four emission spectra have a rather similar intensity. At higher water vol% of 70% and 80%, this green emission band slightly red-shifts to 522 nm, but its intensity decreases significantly. The vibronic emission side-band is still recognizable at around 560 nm in these spectra. However, a new emission band

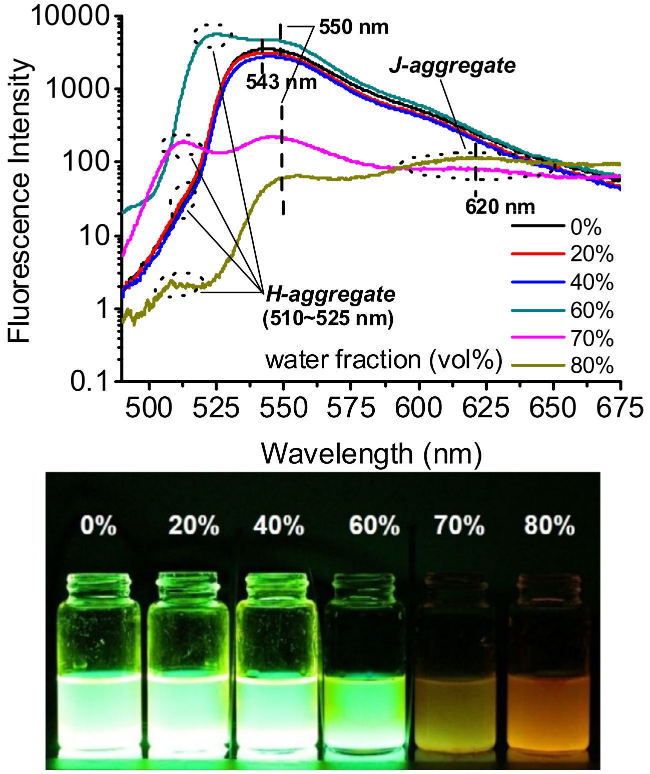

FIGURE 5 Fluorescence spectra (top) and fluorescence photograph (bottom) of **88TPEBODP** in THF solution (10^{-3} M) with various water volume fractions. Fluorescence spectra were recorded with a 480 nm excitation wavelength. Fluorescence photographs were taken under a UV illumination at 366 nm

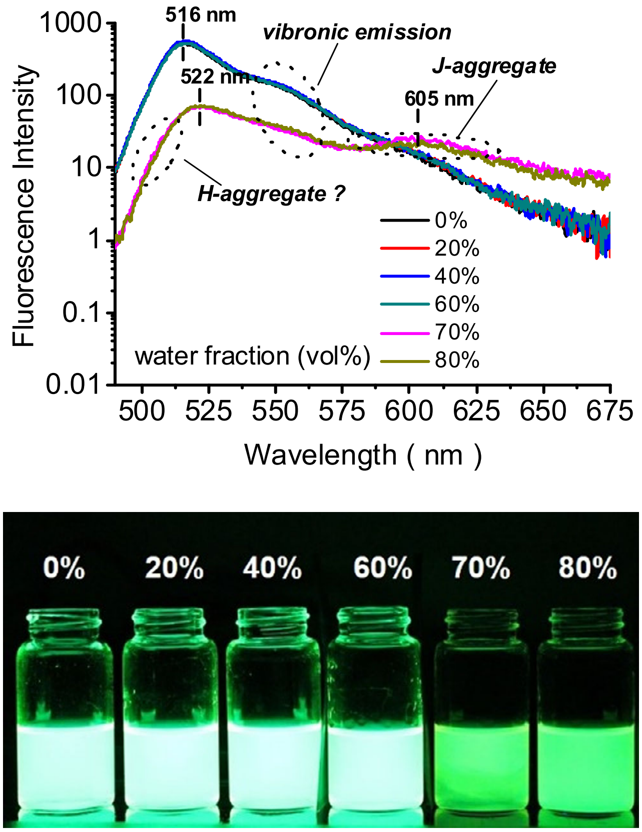

FIGURE 6 Fluorescence spectra (top) and fluorescence photograph (bottom) of **88TPEBODP** in THF solution (10^{-5} M) with various water volume fractions. Fluorescence spectra were recorded with a 480 nm excitation wavelength. Fluorescence photographs were taken under a UV illumination at 366 nm

emerges around 605 nm (Figure 5). Similarly, we attribute the newly emerging emission band to the J-type aggregate of **88TPEBODP**. Presumably, there should be an emission band of around 500–515 nm due to the H-type aggregate of **88TPEBODP**, which is barely distinguishable in the spectra. As the emission spectra are predominated by the λ_{max}^{em} of 522 nm, a greenish color remains in the fluorescence photograph regardless of water vol%, except for a slight yellowish hue of the THF solution with 70% and 80% of water vol % (Figure 6).

From either fluorescence photograph or the emission spectra, 60% (10^{-3} M) or 70% (10^{-5} M) seems to be a common water vol% at which the brightness of the photograph and the intensity of spectra decrease. Similar to what happens for **35TPEBODP**, we infer that this is the water vol% that initiates the formation of a substantial aggregate of **88TPEBODP** in THF solution. Similarly, based on the PL study described here, **88TPEBODP** is an ACQ (not AIE nor AIEE) luminogen. From the solution PL study of **88TPEBODP**, we have observed a color change, which is clearly visible at a high concentration of 10^{-3} M but is less clear at 10^{-5} M. Finally, the multiple emission bands observed for **88TPEBODP** in high water-containing THF solution simply rule out the possibility of TICT, which was used to explain the color change of PL of TPE-containing BODIPY derivatives.[8]

2.3.3 | 26TPEBODP

Unlike those of **35TPEBODP** or **88TPEBODP**, the fluorescence spectra are much simpler at either high or low concentrations. First, with increasing water vol%, the shifting of spectroscopic wavelength (λ_{max}^{em}) is very small, 606–610 nm and 577–583 nm for a high concentration of 10^{-3} M and a low concentration of 10^{-5} M, respectively (Figures 7 and 8). This is consistent with the yellowish orange color in THF solution regardless of water content (vol%). Second, the H-type or J-type aggregate mentioned above for **88TPEBODP** simply does not occur based on the profile of recorded fluorescence spectra. However, the variation of fluorescence intensity is more subtle and requires further elaboration.

For a high-concentration (10^{-3} M) THF solution (Figure 7), the florescence intensity first increases

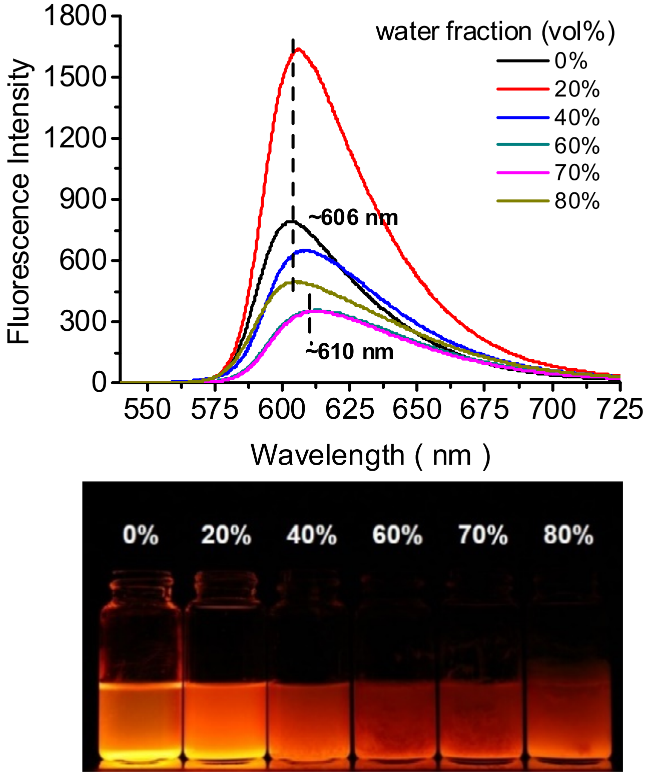

FIGURE 7 Fluorescence spectra (top) and fluorescence photograph (bottom) of **26TPEBODP** in THF solution (10^{-3} M) with various water volume fractions. Fluorescence spectra were recorded with a 480 nm excitation wavelength. Fluorescence photographs were taken under a UV illumination at 366 nm

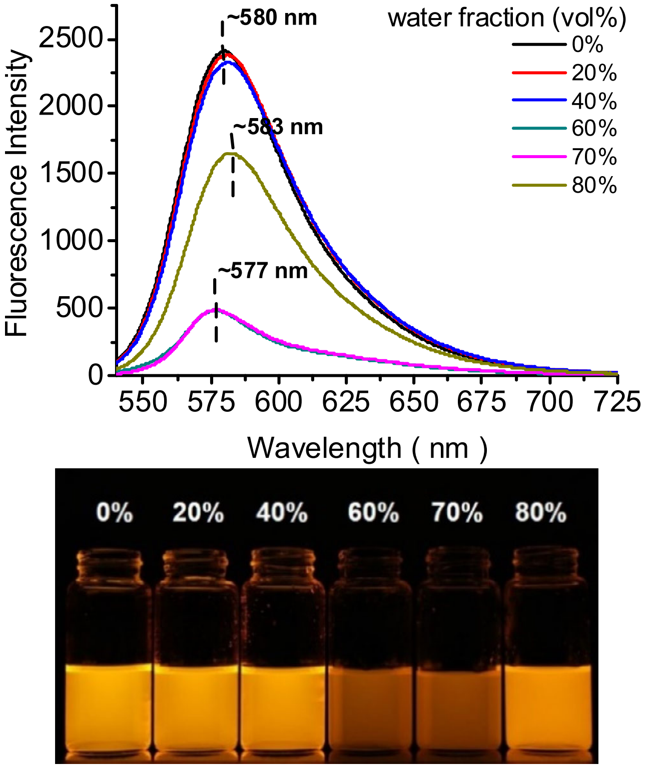

FIGURE 8 Fluorescence spectra (top) and fluorescence photograph (bottom) of **26TPEBODP** in THF solution (10^{-5} M) with various water volume fractions. Fluorescence spectra were recorded with a 480 nm excitation wavelength. Fluorescence photographs were taken under a UV illumination at 366 nm

substantially with 20% of water vol%. This can be explained by the AIEE characteristic of **26TPEBODP**. However, when the water vol% further increases to 40%, the florescence intensity decreases significantly. At first, we infer that ACQ surpasses AIEE at the water vol% of 40%. Nevertheless, the florescence intensity further decreases at water vol % of 60% and 70% but bounces back and beyond at water vol% of 80%. Based on a pertinent literature report,[6] the aggregate formation at the early stage, including water vol% of 40%, 60%, and 70%, has a crystalline nature, and the formation of an amorphous aggregate takes place at a higher water vol% of 80%.

Such a variation of fluorescence intensity is somewhat different when the concentration is lower at 10^{-5} M (Figure 8). The first reduced and then bounced back fluorescence intensity is still there but occurs at a higher water vol % of 60–80% due to a more diluted **26TPEBODP** in the solution. A greater difference was found for high- and low-concentration solutions at low water vol%. Very different from those of high-concentration solutions, the fluorescence intensity of the low-concentration solution remains nearly unchanged at water vol% of 0, 20, and 40%. The plausible AIEE observed for **26TPEBODP** at a high concentration of 10^{-3} M disappears when the solution concentration is lower at 10^{-5} M. Therefore, once again, the solution PL of **26TPEBODP** is concentration dependent, similar to that of **35TPEBODP** and **88TPEBODP**.

2.4 | Fluorescence quantum yields

With the correction of refractive index difference (refractive index of THF solution containing 80 vol% water is 1.350), the solution fluorescence quantum yields were determined relative to that of PM546 (ϕ = 78% in THF)[1] for **PhBODP** and **88TPEBODP**, of H_2TPP (ϕ = 11% in benzene)[14] for **35TPEBODP**, and of rubrene (ϕ = 61% in toluene)[15] for **26TPEBODP**. Table 1 summarizes the fluorescence quantum yield (ϕ) data of BODIPY compounds in solution. For BODIPY compounds in solid state, as powder, or as 5 wt% dopant in PS-hosted thin film, ϕ data were measured by the integrating sphere equipped in a Hitachi fluorescence spectrophotometer F-7000.

First, high-concentration solutions always show lower ϕ than low-concentration solutions, either with or without tethered TPE, regardless the position of tethered-TPE. Such results indicate that the TPE tethering cannot prevent the

TABLE 1 Fluorescence quantum yields of **PhBODP** and three TPEBODP compounds in this study

	$\phi_{\text{solution}}{}^{a}$ (%)	$\phi_{\text{solution}}{}^{b}$ (%)	$\phi_{\text{solid}}{}^{c}$ (%)
	THF solution	THF solution	5 wt%
	80% H_2O vol%	80% H_2O vol%	100 wt%
88TPEBODP	68	59	5
	33	6	2
35TPEBODP	78	30	5
	8	1	1
26TPEBODP	86	24	13
	44	12	6
PhBODP	41	28	3
	8	6	1

[a] 1×10^{-5} M.

[b] 1×10^{-3} M.

[c] In polystyrene (PS) thin film.

fluorescence of BODIPY from concentration quenching. However, in a THF solution of 1×10^{-5} M, all three TPE-tethered BODIPY fluorophores show higher ϕ than **PhBODP**. It is more or less the same in THF solution with a higher concentration of 1×10^{-3} M. Based on these results, TPE tethering seems to be effective in promoting the fluorescence intensity of BODIPY compounds. In THF solution with 80 vol% of water, except for one case, **35TPEBODP** with a concentration of 1×10^{-3} M, all TPE-tethered BODIPY fluorophores exhibit ϕ greater than or similar to the ϕ of **PhBODP**. In this regard, once again, TPE tethering seems to be effective (for enhancing ϕ).

2.5 | Electroluminescence characterization

A series of BODIPY (**PhBODP**, **88TPEBODP**, and **26TPEBODP**) OLEDs have been fabricated based on device configuration of ITO/NPB(35 nm)/TAPC(5 nm)/CBP:BODIPY(x%, 30 nm)/BCP(10 nm)/TPBI(30 nm)/LiF (1 nm)/Al(100 nm). Here, we use NPB, TAPC, CBP, BCP, and TPBI for the hole-transporting layer and electron-blocking layer, host material (for dopant devices), hole-blocking layer, and electron-transporting layer, respectively. The HOMO and LUMO energy levels were estimated by a low-energy photoelectron spectrometer (Riken-Keiki AC-2) and the solid-state onset absorption wavelength (as optical band-gap energy), respectively. Including those of other materials used in OLED fabrication, HOMO and LUMO energy levelsof PhBODP, 88TPEBODP,35TPEBODP, and 26TPEBODP are summarized in Figure 9. The deployment of those blocking layers, TAPC and BCP, in the device is for the purpose of eliminating the EL from the transporting layer of NPB and TPBI, even though the choice of CBP as the host material seems fine in the exciton confinement of BODIPY fluorophores.

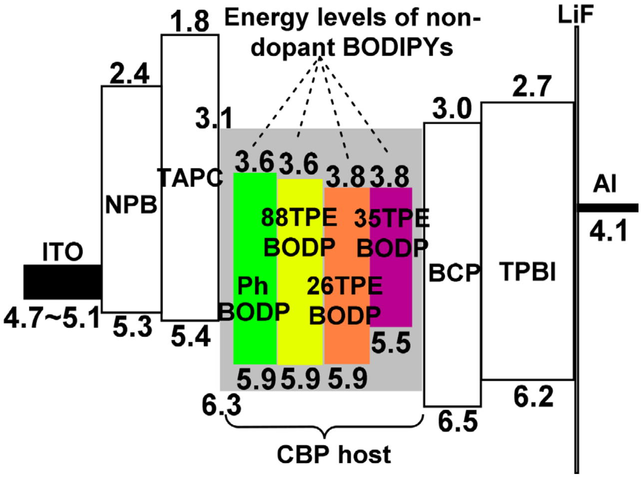

FIGURE 9 Energy level diagram of four BODIPY compounds and materials used in device fabrication

First, comparing EL spectra of the three BODIPY OLEDs, a dual EL has been observed for **PhBODP** OLEDs, having either 50 or 100% dopant concentration, whereas dual EL can be observed only at 100% concentration of **88TPEBODP,** that is, nondopant device (see EL spectra shown in Figure 10). Moreover, a dual EL observed only at 100% dopant concentration of **88TPEBODP** implies that double-tethered TPE on **PhBODP** effectively reduces the aggregation of **PhBODP** and hence the possible excimer emission (at long wavelength), which is consistent with higher ϕ obtained for **88TPEBODP** than **PhBODP** (Table 1). Accordingly, regardless of dopant concentration, **88TPEBODP** OLEDs always show higher external quantum efficiencies (EQEs) than **PhBODP** OLEDs, and the former devices always exhibit much brighter EL (electroluminescence, *L*) than the latter devices (Table 2 and Figure 10). In addition, the very high-driving voltages of **PhBODP** OLEDs have been significantly reduced in **88TPEBODP** OLEDs.

Regarding **26TPEBODP** OLEDs, devices were only observed for a single EL regardless of the dopant concentration. The different EL behavior of dopant concentration dependence is quite consistent with what we observed in the PL study. Furthermore, such a single emission band of EL has a longer wavelength compared with that of **88TPEBODP** or **PhBODP**, and the λ_{max} of EL varies little with different dopant concentrations of 1, 50, and 100 wt%, although the EL bandwidth becomes larger (Figure 10). Similar to the PL, the EL of **26TPEBODP** is rather different from that of **88TPEBODP**. As the determined ϕ of **26TPEBODP** is the highest (86% in diluted THF, 13% in 5 wt% PS thin film, and 6% as solid powder) compared with

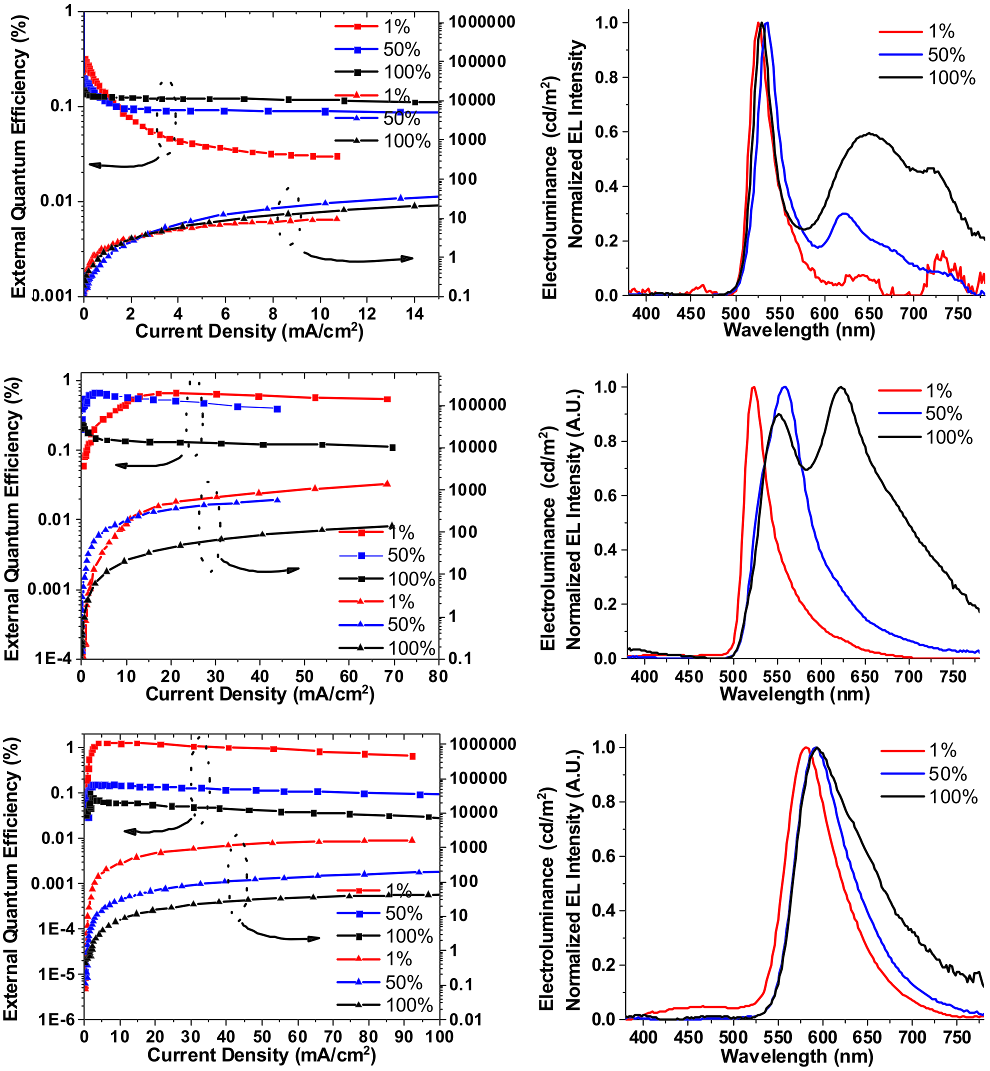

FIGURE 10 Electroluminescence characteristics of **PhBODP** (top row figures), **88TPEBODP** (middle row figures), and **26TPEBODP** (bottom row figures)

TABLE 2 Electroluminescence characteristics of OLEDs fabricated with four BODIPY compounds in this study

Device	DC[a] (%)	EQE, voltage[b] (%, V)	*L*, voltage[c] (cd/m^2, V)	λ_{EL}[d] (nm)	CIE[d] (*x*, *y*)
PhBODP	1	0.32 (23.0)	1.1, 9 (35.0)	526	(0.27, 0.67)
	10	0.38 (20.0)	1.2, 24 (35.0)	528	(0.31, 0.65)
	50	0.20 (20.0)	1.1, 77 (31.5)	536, 622	(0.39, 0.59)
	100	0.15 (10.2)	1.7, 108(17.0)	530, 650	(0.43, 0.55)
88TPE BODP	1	0.67 (13.0)	517, 1,359 (15.0)	524	(0.29, 0.64)
	10	0.51 (9.0)	40, 268 (15.0)	526	(0.30, 0.65)
	50	0.67 (10.0)	61, 569 (15.0)	558	(0.42, 0.56)
	100	0.24 (7.5)	3, 140 (12.0)	552, 622	(0.50, 0.48)
26TPE BODP	1	1.30 (10.5)	231, 1,603 (15.0)	582	(0.50, 0.44)
	10	0.27 (14.0)	4, 15 (17.0)	588	(0.55, 0.43)
	50	0.16 (13.5)	7, 256 (25.5)	592	(0.56, 0.42)
	100	0.10, (9.5)	1, 48 (21.0)	594	(0.58, 0.41)

[a] Dopant concentration.

[b] Maximum EQE, driving voltage.

[c] Electroluminance at maximum EQE, maximum *L*, and driving voltage.

[d] At maximum *L*.

those of either **PhBODP** or **88TPEBODP** (Table 1), **26TPEBODP** OLEDs with 1 wt% of dopant concentration display the best EQE of 1.3% and the most intense EL of approximately 1,600 cd/m^2 (Table 2 and Figure 10).

During the nondopant device fabrication, we have observed that the deposition rate of **PhBODP** and **88TPEBODP** fluorophores has a different effect on the promotion of molecular aggregation and hence the long wavelength excimer emission (Figure 11 and Table 3). Although a slower deposition rate promotes the long wavelength EL of **88TPEBODP**, it is the faster deposition rate that enhances the long wavelength EL of **PhBODP**. We may reasonably surmise that such an opposite dependence of deposition rate must be due to the chemical structure of tethered TPE, which alters the molecule-stacking interaction of BODIPY fluorophores.

3 | CONCLUSIONS

We have comprehensively studied both PL and EL of three double TPE-tethered **PhBODP** fluorophores. We have found that the solution PL (wavelength and intensity) of these TPE-tethered BODIPY depends on the solution concentration and the chemical position of these tethered

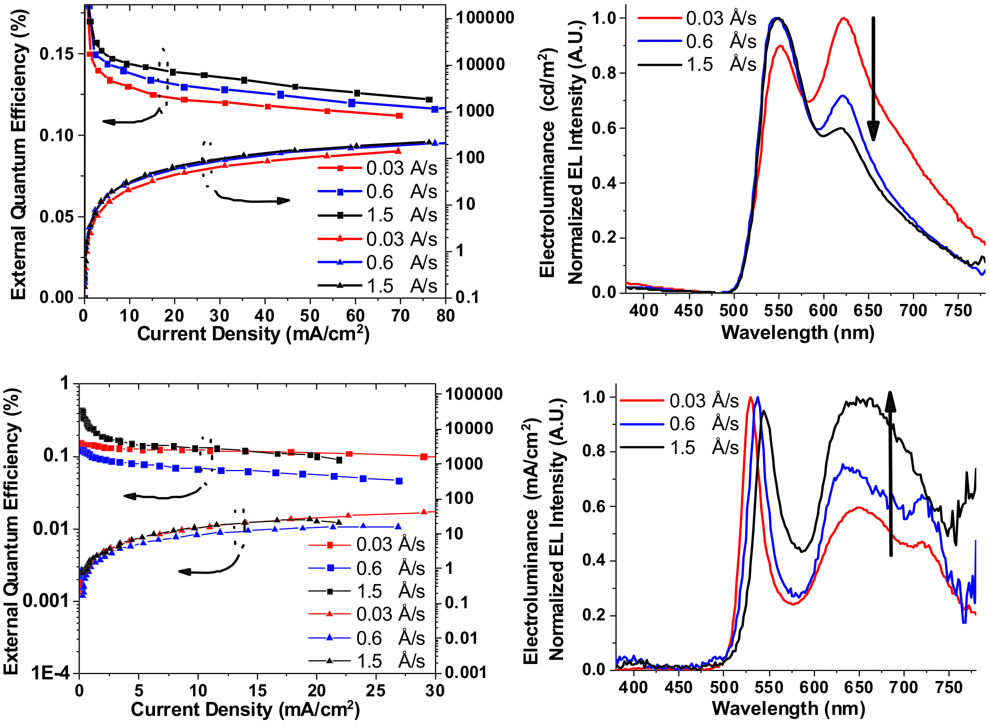

FIGURE 11 Electroluminescence characteristics of **88TPEBODP** (top row figures) and **PhBODP** (bottom row figures) nondopant OLED, with variable deposition rates, 0.01, 0.6, and 0.15 Å/s

TABLE 3 Electroluminescence characteristics of OLEDs fabricated with nondopant **88TPEBODP** and **PhBODP** with variable deposition rates

Device	DR[a] (Å/s)	EQE,[b] voltage (%, V)	*L*[c] (cd/m^2, V)	λ_{EL}[d] (nm)	CIE[d] (*x*, *y*)
88TPE BODP	0.03	0.15 (7.5)	2.5, 140 (12.0)	552, 622	(0.50, 0.48)
	0.6	0.21 (6.0)	1.3, 288 (12.0)	546, 620	(0.46, 0.52)
	1.5	0.19 (6.0)	1.6, 218 (12.0)	550, 620	(0.46, 0.52)
Ph BODP	0.03	0.15 (7.5)	1.7, 108 (17.0)	530, 650	(0.42, 0.55)
	0.6	0.12 (13.0)	1.5, 16 (20.5)	538, 638	(0.46, 0.51)
	1.5	0.43 (12.0)	1.4, 26 (21.0)	544, 648	(0.50, 0.48)

[a] Deposition rate.

[b] Maximum EQE, driving voltage in parenthesis.

[c] Electroluminance at maximum EQE, maximum *L*, and driving voltage in parenthesis.

[d] At maximum *L*.

TPE. Nevertheless, through the determination of PL quantum yields of THF and water (80 vol%)–THF solution, we have demonstrated that none of these TPE-tethered BODIPY fluorophores exhibits AIE or AIEE. However, the double-tethered TPE BODIPY fluorophores, that is, **88TPEBODP**, **35TPEBODP**, and **26TPEBODP**, do have an enhanced ϕ in diluted THF solution and in 5 wt% PS thin film compared with those of **PhBODP**. Therefore, we have observed that 1 wt% dopant OLEDs of **88TPEBODP** and **26TPEBODP** all show higher EQE and brighter EL than those of **PhBODP** OLEDs. Finally, due to the low ϕ of these BODIPY fluorophores in solid state or dopant PS thin film, none of the OLEDs fabricated in this study exhibits satisfactory EQE.

4 | EXPERIMENTAL

4.1 | General

^{1}H and ^{13}C NMR spectra were measured on a Bruker AV-400 MHz NMR Fourier transform spectrometer at room temperature. Electron ionization (EI) or fast atom bombardment (FAB) mass spectroscopy (MS) were performed by the Mass Spectroscopic Laboratory, an in-house service of the Institute of Chemistry, Academic Sinica. Elemental analyses were performed by the Instrumentation Center, National Taiwan University. Thermal decomposition temperatures (T_d's) of the BODIPY compounds were measured by thermogravimetric analysis (TGA) using Perkin-Elmer TGA-7 analyzer systems. UV–visible absorption spectra were recorded on a Hewlett-Packard 8453 diode array spectrophotometer. Room temperature fluorescence spectra were recorded on a Hitachi fluorescence spectrophotometer F-7000. The measurement of solution and solid-state photoluminescence quantum yields (PLQYs) was also carried out by F-7000. The ionization potentials (or HOMO energy levels) of the BODIPY compound in this study were determined using a low-energy photoelectron spectrometer (Riken-Keiki AC-2). A microwave synthesizer (CEM Discover SP) with an irradiation power of 150 W was set to 140°C on a reaction vessel of about 20 mL.

4.2 | Synthesis of 3,5-dibromobenzaldehyde

At −78°C, to a solution of 1,3,5-tribromobenzene (2 g, 6.4 mmol) in diethyl ether (33 mL), *n*-butyllithium (4 mL, 6.4 mmol, 1.6 M in hexane) was slowly added. The mixture was stirred for 30 min under nitrogen atmosphere. After the slow addition of a mixture of DMF (1 mL, 12.8 mmol) and diethyl ether (1.35 mL), the reaction solution was stirred for a further 60 min and then gradually warmed up to 0°C. The reaction was quenched with a 2 N hydrochloric acid aqueous solution, extracted with chloroform, dried over magnesium sulfate, and subjected to purification by column chromatography (silica gel, hexanes). A white solid was obtained with isolated yields of 60% (1.01 g). ^{1}H NMR (400 MHz, $CDCl_3$): δ 9.878 (s, 1H), 7.915 (s, 2H), 7.896 (s, 1H). ^{13}C NMR (100 MHz, $CDCl_3$): δ 189.12, 139.57, 138.92, 131.19, 123.94. MS (EI) *m/z* 261.9 (M^+).

4.3 | Synthesis of 3,5-bis(2,4,4,5,5-pentamethyl-1,3,2-dioxaborolan-2-yl)benzaldehyde

A flask charged with 3,5-dibromobenzaldehyde (0.50 g, 1.90 mmol), bis(pinacolato)diboron (1.10 g, 4.18 mmol), $PdCl_2$(dppf) (0.07 g, 0.095 mmol), and KOAc (1.20 g, 12.5 mmol) in 1,4-dioxane (16 mL) was stirred at a refluxing temperature for 21 h under a nitrogen atmosphere. After cooling, the solution mixture was filtered through a short pad of celite, evaporated under reduced pressure. The residue was redissolved in a mixture of ethyl acetate and water and then extracted three times with water. After drying over magnesium sulfate, the organic solution was subjected to purification by column chromatograph with silica gel (dichloromethane/hexanes, 1/5) to afford a green solid with yields of 88% (0.60 g). ^{1}H NMR (400 MHz, $CDCl_3$): δ 10.03 (s, 1H), 8.46 (s, 1H), 8.37 (s, 2H), 1.33 (s, 24H). ^{13}C NMR (100 MHz, $CDCl_3$): δ 192.61, 146.83, 138.79, 135.10, 84.21, 24.87. MS (EI) *m/z* 359.3 ($M + H^+$).

4.4 | Synthesis of 3,5-bis(1,2,2-triphenylvinyl)benzaldehyde

To a mixture of 3,5-bis(2,4,4,5,5-pentamethyl-1,3,2-dioxaborolan-2-yl)benzaldehyde (0.40 g, 1.12 mmol) and bromotriphenylethylene (1.20 g, 3.58 mmol), $PdCl_2$(dppf) (0.040 g, 0.056 mmol), a mixture of 1,4-dioxane (15.6 mL) and K_3PO_4 (1.80 g, 8.40 mmol) was added. The reaction mixture was stirred at 80°C for 16 hr under a nitrogen atmosphere. After cooling, the solution mixture was filtered through a short pad of celite, evaporated under reduced pressure. The residue was redissolved in a mixture of dichloromethane and water and then extracted three times with water. After drying over magnesium sulfate, the organic solution was subjected to purification by column chromatograph with silica gel (dichloromethane/hexanes, 1/3) to afford a pale yellow solid with yields of 36% (0.24 g). ^{1}H NMR (400 MHz, $CDCl_3$): δ 9.61 (s, 1H), 7.25 (d, $J = 1.6$ Hz, 2H), 7.13–7.03 (m, 17H), 6.97 (t, $J = 1.6$ Hz, 1H), 6.93–6.89 (m, 8H), 6.75–6.72 (m, 4H).^{13}C NMR

(100 MHz, $CDCl_3$): δ 192.20, 144.55, 143.06, 142.77, 142.28, 141.94, 140.17, 139.41, 135.89, 131.26, 131.01, 130.90, 130.36, 127.72, 127.65, 126.65, 126.60. HRMS (FAB) *m/z* calcd for $C_{47}H_{34}O$ 614.2610, found 614.2613 (M^+). Anal. calcd for $C_{47}H_{34}O$: C 91.82, H 5.57; found: C 90.83, H 5.48.

4.5 | Synthesis of 8-(3,5-bis((1,2,2-triphenylvinyl)phenyl)-4,4-difluoro-1,3,5,7-tetramethyl-4-bora-3*a*,4*a*-diaza-*s*-indance, 88TPEBODP

To a deoxygenated solution of 3,5-bis(1,2,2-triphenylvinyl) benzaldehyde (0.60 g, 0.97 mmol) and 2,4-dimethylpyrrole (0.20 g, 2.21 mmol) in dichloromethane (250 mL), trifluoroacetic acid was added (one drop). The mixture was stirred under a nitrogen atmosphere at room temperature for 8 hr. The resulting dark orange solution was treated with 2,3-dichloro-5,6-dicyano-1,4-benzoquinone (0.33 g, 1.36 mmol) and stirred at room temperature for 2 hr. Then, triethylamine (5.3 mL) and boron trifluoride diethyl etherate (5.3 mL) were added, and the mixture was stirred for another hour. After washing with water, the organic phase was separated, dried over magnesium sulfate, and subjected to purification by column chromatography (silica gel, ethyl acetate/hexanes: 1/7). An orange solid was obtained with isolated yields of 45% (0.36 g). ^1H NMR (400 MHz, $CDCl_3$): δ 7.16–7.14 (m, 6H), 7.03–7.00 (m, 16H), 6.89–6.88 (m, 4H), 6.83 (s, 1H), 6.72–6.71 (d, J = 1.2 Hz, 2H), 6.68–6.66 (m, 4H), 5.86 (s, 2H), 2.45 (s, 6H), 1.25 (s, 6H). ^{13}C NMR (100 MHz, $CDCl_3$): δ 155.25, 144.66, 143.39, 143.04, 142.75, 142.64, 141.56, 141.43, 140.15, 135.04, 134.55, 131.30, 130.95, 130.81, 128.49, 127.92, 127.66, 127.61, 126.55, 120.83, 15.57, 14,47. HRMS (FAB) *m/z* calcd for $C_{29}H_{27}BF_2N_2O$ 832.3800, found 832.3807 (M^+). Anal. calcd for $C_{29}H_{27}BF_2N_2$: C 85.09, H 5.69, N 3.36; found: C 84.28, H 5.60, N 3.30.

4.6 | Synthesis of 3,5-bis(1,2,2-triphenylvinyl)-4,4-difluoro-1,7-dimethyl-8-phenyl-4-bora-3*a*,4*a*-diaza-*s*-indance, 35TPEBODP

To a solution of 4-(1,2,2-triphenylvinyl)benzaldehyde (0.44 g, 1.23 mmol) and **PhBODP** (0.10 g, 0.31 mmol) in DMF (7.7 mL), six drops of acetic acid and piperidine trifluoroacetic acid were added. The solution was deoxygenated by purging in an argon atmosphere for 30 min. The reaction of the solution was carried out by microwave heating (150 W) set at 140°C for 5 min. The solvent and volatile organics were removed under reduced pressure. The residue was redissolved in a mixture of dichloromethane and water and then extracted three times with water. After drying over magnesium sulfate, the organic solution was subjected to purification by column chromatograph with silica gel (dichloromethane/hexanes, 1/2) to afford a dark green solid with yields of 36% (0.11 g). ^1H NMR (400 MHz, $CDCl_3$): δ 7.62 (d, J = 16.0 Hz, 2H), 7.47–7.45 (m, 3H), 7.34–7.29 (m, 6H), 7.13–7.00 (m, 36H), 6.56 (s, 2H), 1.40 (s, 6H). ^{13}C NMR (100 MHz, $CDCl_3$): δ 152.57, 144.68, 143.68, 143.60, 143.54, 141.96, 141.51, 140.55, 138.56, 135.85, 135.19, 134.69, 133.45, 131.80, 131.42, 131.34, 129.04, 128.93, 128.48, 127.85, 127.71, 127.61, 126.91, 126.72, 126.53, 126.47, 119.00, 117.75, 14.56. HRMS (FAB) *m/z* calcd for $C_{73}H_{55}BF_2N_2$ 1,008.4426, found 1,008.4436 (M^+). Anal. calcd for $C_{29}H_{27}BF_2N_2$: C 86.89, H 2.78, N 5.49; found: C 85.80, H 5.38, N 2.78.

4.7 | OLED fabrication and EL characterization

OLED devices were fabricated by vacuum–thermal deposition using Sumimoto Cryogenics at a chamber pressure of 10^{-6} Torr. The ITO substrate was purchased from Ruilong with sheet resistance of around 30 Ω/sq. Host material CBP (4,4′-bis[*N*-carbazolyl]-2,2′-biphenyl), TAPC (di-[4-[*N*,*N*-ditolylamino]phenyl]cyclohexane), and BCP (2,9-dimethyl-4,7-diphenyl-1,10-phenanthroline) were purchased from Lumtec. NPB (1,4-bis[1-naphthylphenylamino]biphenyl) and TPBI (2,2′,2″-[1,3,5-phenylene]tris[1-phenyl-1*H*-benzimidazole]) were prepared via published methods. For the cathode of devices, an ultrathin LiF (1 nm) interfacial layer and then aluminum (100 nm) were vacuum–thermal deposited. The effective size of the emitting diode was 3.14 mm^2. The current density and voltage characteristics were measured by a dc current/voltage source meter (Keithley 2400), and the device brightness (or electroluminescence, cd/m^2) and EL spectra were monitored and recorded with a spectrophotometer (PR670; Photo Research).

ACKNOWLEDGMENTS

We thank the Ministry of Science and Technology (MOST 106-2113-M-001-016-MY3), iMATE Program of Academia Sinica, and National Chiao Tung University.

REFERENCES

[1] F. L. Arbeloa, T. L. Arbeloa, I. L. Arbeloa, *J. Photochem. Photobiol.* **1999**, *121*, 177.

[2] Z. Zhao, J. W. Y. Lam, B. Z. Tang, *Curr. Org. Chem.* **2010**, *14*, 2109.

[3] Z. Zhao, J. W. Y. Lam, B. Z. Tang, *J. Mater. Chem.* **2012**, *22*, 23726.

[4] R. Hu, C. F. A. Gómez-Durán, J. W. Y. Lam, J. L. Belmonte-Vázquez, C. Deng, S. Chen, R. Ye, E. Peña-Cabrera, Y. Zhong, K. S. Wong, B. Z. Tang, *Chem. Commun.* **2012**, *48*, 10099.

[5] Z. Li, Y. Chen, X. Lv, W.-F. Fu, *New J. Chem.* **2013**, *37*, 3755.

[6] M. Baglan, S. Ozturk, B. Gür, K. Meral, U. Bozkaya, O. A. Bozdemir, S. Atilgan, *RSC Adv.* **2013**, *3*, 15866.

[7] Z. Zhao, B. Chen, J. Geng, Z. Chang, L. Aparicio-lxta, H. Nie, C. C. Goh, L. G. Ng, A. Qin, G. Ramos-Ortiz, B. Liu, B. Z. Tang, *Part. Part. Syst. Charact.* **2014**, *31*, 481.

[8] C. F. A. Gomez-Duran, R. Hu, G. Feng, T. Li, F. Bu, M. Arseneault, B. Liu, E. Peña-Cabrera, B. Z. Tang, *ACS Appl. Mater. Interfaces* **2015**, *7*, 15168.

[9] S. Baysec, A. Minotto, P. Klein, S. Poddi, A. Zampetti, S. Allard, F. Cacialli, U. Scherf, *Sci. China Chem.* **2018**, *61*, 932.

[10] R. Hu, E. Lager, A. Aguilar-Aquilar, J. Liu, J. W. Y. Lam, H. H. Y. Sung, I. D. Williams, Y. Zhong, K. S. Wong, E. Peña-Cabrera, B. Z. Tang, *J. Phys. Chem. C* **2009**, *113*, 15845.

[11] A. Vázquez-Romero, N. Kielland, M. J. Arévalo, S. Preciado, R. J. Mellanby, Y. Feng, R. Lavilla, M. Vendrell, *J. Am. Chem. Soc.* **2013**, *135*, 16018.

[12] B. Xu, W. Li, J. He, S. Wu, Q. Zhu, Z. Yang, Y.-C. Wu, Y. Zhang, C. Jin, P.-Y. Lu, Z. Chi, S. Liu, J. Xu, M. R. Bryce, *Chem. Sci.* **2016**, *7*, 5307.

[13] T. Yoshida, L. Ilies, E. Nakamura, *ACS Catal.* **2017**, *7*, 3199.

[14] P. G. Seybold, M. Gouterman, *J Molec Spectr* **1969**, *31*, 1.

[15] G. Laurent, N. T. Ha-Duong, R. Meallet-Renault, R. B. Pansu, *Handai Nanophoton* **2004**, *1*, 89.

AUTHOR BIOGRAPHIES

Mr Chiun-Jen Yang graduated from the Department of Chemistry, Fu Jen Catholic University, with a BS in 2017. He then entered the Department of Applied Chemistry, National Chiao Tung University, as an MS student. Chiun-Jen's research focuses on the organic synthesis and physical characterization of fluorescence materials for organic light-emitting diodes or bioimaging application.

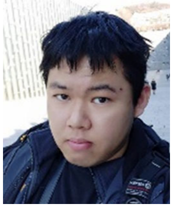

Mr Jian Haur Lee was born in Negeri Sembilan, Malaysia. He received his MS degree in chemistry from National Chiao Tung University in 2018. He is currently a research assistant in Chen's group at the Institute of Chemistry, Academia Sinica. His research mainly focused on the material design and synthesis of organic light-emitting diodes, including host materials and luminescence materials. His interest also includes the discussion on the possibility of fabricating the materials into optoelectronics devices.

Since 2003, Dr Chin-Ti Chen has been a Research Fellow at the Institute of Chemistry, Academia Sinica. He received his PhD from the University of Illinois at Urbana-Champaign in 1992. Dr Chen has worked as a Postdoctoral Research Fellow at the California Institute of Technology in 1992–1995. In 1995, he moved to the Institute of Chemistry, Academia Sinica as an Assistant Research Fellow, promoted to Associate Research Fellow in 2000. His research interests include organic materials for optoelectronics applications, such as perovskite solar cells (PVSCs), organic photovoltaic (OPVs), and organic light-emitting diodes (OLEDs).

How to cite this article: Yang C-J, Lee JH, Chen C-T. Synthesis, photoluminescence, and electroluminescence characterization of double tetraphenylethene-tethered BODIPY luminogens. *J Chin Chem Soc*. 2019;1–12. https://doi.org/10.1002/jccs.201900163